

Design Considerations to Scale up Vacuum Thermal Stripping for Ammonia Recovery from Anaerobic Digestate

Wendong Tao^{1*}, Anayo T. Ukwuani¹

¹Department of Environmental Resources Engineering, College of Environmental Science and Forestry, State University of New York, Syracuse, NY 13210, USA

*Corresponding author. Email: wtao@esf.edu; Telephone: 1(315) 470-4928; Fax: 1(315) 470-6928

Abstract

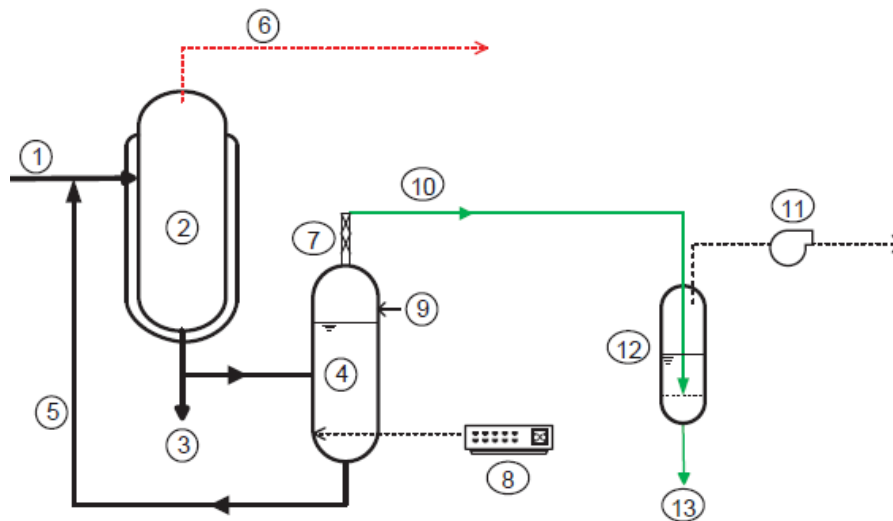
Anaerobic digestion can be inhibited by ammonia at high organic loading rates. When the concentration of ammonia in digestate is reduced by ammonia recovery in a recirculation line, more biogas can be produced at an increased organic loading rate. To facilitate scale-up application of an ammonia recovery process through vacuum thermal stripping coupled with acid absorption, this study investigated the effects of feed depth on vacuum thermal stripping of ammonia in a pilot system, sodium hydroxide dose required to raise feed pH, and thermal stability of the crystals recovered as ammonium sulfate. As feed depth was increased from 8.5 to 25.5 cm, ammonia mass transfer coefficient decreased while the mass of ammonia stripped increased. It appears that 17 cm is a better feed depth than 8.5 and 25.5 cm. Detailed economic analysis is needed to identify the optimum feed depth for a given application. Digested sludge had a greater ammonia mass transfer coefficient than digested dairy manure at each feed depth, which could be attributed to the difference in dissolved solids concentration. Sodium hydroxide doses for the digested dairy manure were higher than those for the digested sludge and co-digested foodwaste. The doses had strong correlations with concentrations of total dissolved solids and ammonia. Both the measured melting points of the recovered crystals and the thermal decomposition profiles resembled those of reagent grade crystals, confirming the production of ammonium sulfate as high-purity crystals.

Keywords: Ammonia recovery, ammonium sulfate, gas absorption, mass transfer, pH elevation, vacuum thermal stripping

1 INTRODUCTION

Anaerobic digestion of protein-rich organic wastes faces process instability issue at high organic loading rates due to accumulation of ammonia and subsequent inhibition to acetoclastic methanogens [1-3]. Recently, a vacuum thermal stripping – acid absorption process was invented to recover ammonia from digestate [4]. When the ammonia recovery process is installed in a recirculation line of an anaerobic digester (Fig. 1), the digester could be loaded at a higher rate while maintaining stable

operation. Meanwhile, the recirculation transforms the energy-intensive thermal stripping process into a profitable ammonia recovery process [5].



- ① Digester feed; ② Anaerobic digester; ③ Digester effluent; ④ Vacuum stripper;
 ⑤ Recirculation of stripped digestate; ⑥ Biogas; ⑦ Demister; ⑧ Temperature controller;
 ⑨ Sodium hydroxide addition; ⑩ Stripped ammonia; ⑪ Vacuum pump; ⑫ Gas absorption column; ⑬ Collection of ammonium sulfate crystals

Fig. 1 Application scheme of the vacuum thermal stripping – acid absorption process for ammonia recovery from anaerobic digestate

When applying vacuum to an enclosed stripper with heated digestate or wastewater, the feed boils at a temperature below the normal boiling point of water. The optimum boiling point for stripping ammonia has been determined to be 65 °C and 28 kPa [4]. Vapor bubbles form in the feed when vapor pressure overcomes the headspace pressure, triggering ammonia mass transfer from liquid to gas phase and finally out of the feed. The vacuum is maintained by a vacuum pump connected to a gas absorption column holding a dilute sulfuric acid solution (Fig. 2). The suction effect of the vacuum enhances transport of the stripped ammonia to the gas absorption column. The stripped ammonia is absorbed to the acid solution for production of ammonium sulfate or $(\text{NH}_4)_2\text{SO}_4$. When the acid solution becomes saturated with $(\text{NH}_4)_2\text{SO}_4$, further reaction of ammonia with sulfuric acid forms long, white $(\text{NH}_4)_2\text{SO}_4$ crystals. A demister is installed between the stripper and absorption column to retain water droplets and mists while free ammonia is transported through it. A vacuum regulator is used to control the gas current that drives slow mixing for granulation of ammonium sulfate crystals in the absorption column.

Ammonia is continuously stripped out of a feed solution until equilibrium is reached between the liquid and gas phases in a batch-operated stripper. Liquid turbulence is enhanced by vapor generation at the heating tube surfaces, thus increasing ammonia mass transfer. Vapor bubble formation deeper in the liquid requires a higher vapor pressure, and thus ammonia mass transfer becomes slower as feed depth is increased. Mechanical mixing could not resolve this barrier. In scale-up applications, feed depth is a critical design parameter that regulates the hydraulic capacity of a stripper and

affects operational costs. This study investigated the effects of feed depth on ammonia stripping efficiency and mass transfer coefficient with a pilot-scale vacuum thermal stripping – acid absorption system.

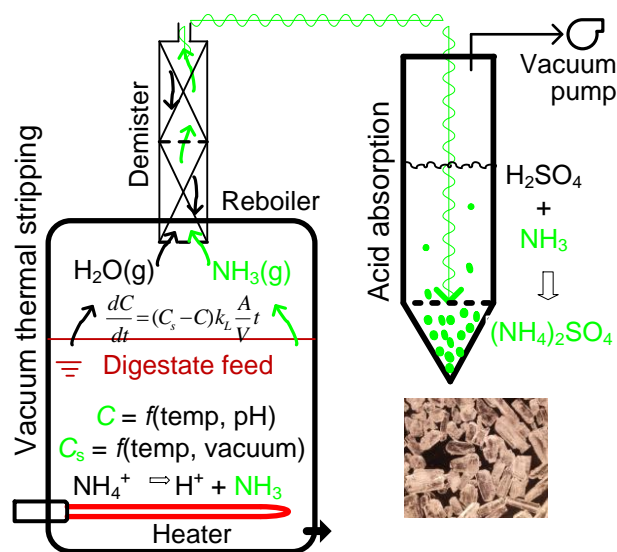


Fig. 2 Sketch of vacuum thermal stripping - acid absorption process for ammonia recovery from anaerobic digestate

Ammonia in digestate exists in aqueous ammonium (NH_4^+) and free ammonia (NH_3), depending on pH and temperature. At pH 9 and the stripping temperature of 65°C , free ammonia accounts for 92% of total ammonia in molar concentrations. Further increase in pH at 65°C results in little increase in the fraction of free ammonia [6], but increases operational costs. Initial feed pH can hence be adjusted to 9 for each batch of vacuum thermal stripping. To facilitate design and economic analysis for commercial application of the vacuum thermal stripping – acid absorption process, sodium hydroxide dosing curves were developed for digested sludge, digested dairy manure, and co-digested foodwaste.

Ammonia has been recovered from digestate and wastewater typically in ammonium sulfate solutions [7-11], although recent studies have explored ways to produce a solid product [4, 6]. Compared with solutions, solid products are more convenient and cost less to store and transport. Ammonium sulfate crystals can be sold as a nitrogen and sulfur fertilizer or reagent grade chemical, thus generating revenues while removing nitrogen. Volatile organic compounds have not been detected in the recovered crystals although being found in spent acid solutions [4]. Nevertheless, the stripped ammonia may be absorbed to the acid solution and form not only $(\text{NH}_4)_2\text{SO}_4$, but also NH_4HSO_4 (ammonium bisulfate), $(\text{NH}_4)_2\text{CO}_3 \cdot \text{H}_2\text{O}$ (ammonium carbonate), NH_4HCO_3 (ammonium bicarbonate), or $(\text{NH}_4)_3\text{H}(\text{SO}_4)_2$ (triammonium hydrogen disulfate), depending on sulfuric acid content and $(\text{NH}_4)_2\text{SO}_4$ saturation condition of the acid solution as well as vacuum regulation [4, 12]. To facilitate market placement and economic analysis, this study verified the chemical composition of the recovered crystals by assessing thermal stability of the recovered crystals.

2 MATERIALS AND METHODS

2.1 Experimental Setup

The pilot-scale ammonia recovery system [4] was operated by a batch mode for vacuum thermal stripping and acid absorption of ammonia in anaerobic digestate at the optimum boiling point combination of temperature 65 °C and vacuum pressure 28 kPa. It had a vacuum stripper connected by a vacuum pump to a gas absorption column. The stripper consisted of a kettle reboiler and a demister, employing single-stage thermal stripping. The kettle reboiler was built with a 40-L stainless steel vacuum vessel (ID 30.5 cm; height 56 cm) and two electric immersion heaters (1.5 kW). Feed temperature was regulated and recorded by a J-Kem Model 250 temperature controller via a J-type thermocouple. The demister was a stainless steel pipe packed with polypropylene mesh (inner diameter 5.08 cm; length 34.3 cm). The absorption column was built with a cylindrical, clear PVC pipe (ID 10 cm; height 50 cm) and a drain valve at the bottom. The PVC pipe is smooth and resistant to sulfuric acid and inorganic salts.

2.2 Batch Stripping Tests at Different Feed Depths

Batch stripping experiments were conducted at feed depths of 8.5, 17.0 and 25.5 cm with anaerobically digested dairy manure collected at a dairy farm located in Cayuga County of New York State and municipal sludge collected from Metropolitan Syracuse Wastewater Treatment Plant in Syracuse, New York, USA. Batch stripping experiments will further be conducted at feed depths of 33.5 and 41.5 cm with the digested sludge. The batch experiments were replicated 5 times at each feed depth (except for single experiments at the depths of 17.0 and 25.5 cm with the digested manure). Feed pH was initially adjusted to 9 and measured at the end of each batch. 1.5 L of 2N sulfuric acid solution was added to the absorption column and used for 3-4 batches of stripping. Once feed temperature reached 65 °C, it was considered to be the start of vacuum thermal stripping and the stripping lasted for 5 h. Feed samples were taken initially and at the end of each batch for determination of total ammonia nitrogen (TAN) concentration with a QuickChem 8500 series automatic flow injection analyzer (LaChat Instruments, Loveland, Colorado, USA), following Standard Method flow injection analysis [13]. For ammonia analysis, liquid samples were collected upon centrifugation of the feed samples at 2500 g for 20 min. Free ammonia concentration was estimated with the measured pH, temperature, and TAN concentration. Feed volume remaining was measured at the end of each batch. The effects of feed depth on stripping of ammonia were evaluated by analysis of variance (ANOVA) for ammonia stripping efficiency (Equation 1), mass of ammonia stripped, and ammonia mass transfer coefficient (Equation 2) [4]. A difference between any pair of feed depths is considered to be significant when P value is less than 0.05.

$$R_e = (C_o \times V_o - C_e \times V_e) \times 100 / (C_o \times V_o) \quad (1)$$

$$\ln \left(\frac{C' - C_s}{C'_o - C_s} \right) = -K_L a t \quad (2)$$

where R_e = ammonia stripping efficiency (%); C_o , C_e = concentration of TAN in feed initially and at the end of a batch (mg/L); V_o , V_e = feed volume initially and at the end of a batch (L); $K_L a$ = volumetric liquid mass transfer coefficient (1/h); C'_o , C' = concentration of free ammonia in feed initially and at time t (mg/L); and C_s = ammonia saturation concentration in liquid (mg/L).

2.3 Developing Dosing Curves for pH Elevation

Both caustic soda and lime are low-cost chemicals to raise pH. Unlike lime that results in chemical sludge, caustic soda is preferred for pH elevation. Caustic soda dosing curves were developed for three common types of digestate, i.e., digested municipal sludge, digested dairy manure, and co-digested food waste and dairy manure. Samples (100-150 mL each) were titrated with a 5N NaOH solution to pH over 11. Four samples for each type of digestate collected on different dates were titrated. The variations of cumulative dosage with pH were fitted with polynomial equations so as to estimate the total dose to raise pH to 9 and the dose to increase pH from 8 to 9. In order to assess the influence of ammonia and solids concentrations on pH response to NaOH dose, each sample was analyzed for concentrations of total solids, total dissolved solids, and TAN. Determination of total solids concentration followed the Standard Method [13]. Total dissolved solids concentration was measured with a portable meter (HQ40d, Hach Company, Loveland, Colorado, USA). TAN concentration was determined as mentioned in Section 2.2.

2.4 Thermal Analysis of Recovered Crystals

The crystals recovered earlier from foodwaste digestate and reverse osmosis retentate of landfill leachate [4] were sampled for determination of thermal stability with reference to that of reagent grade ammonium sulfate crystals (Ward's Science, St. Catharines, Ontario, Canada). The impurity was attributed to NH_4HSO_4 , $(\text{NH}_4)_2\text{CO}_3 \cdot \text{H}_2\text{O}$, NH_4HCO_3 , and $(\text{NH}_4)_3\text{H}(\text{SO}_4)_2$. Melting point and thermal decomposition were examined to confirm the purity of the recovered crystals.

The melting temperature of the recovered crystals was determined by differential scanning calorimetry (DSC). Samples (7.1–8.1 mg each) of the crystals were loaded into a Tzero™ aluminum pan and heated to 340 °C at a heating rate of 10 °C/min. Heat flow analysis was performed under a nitrogen atmosphere with a nitrogen flow rate of 50 mL/min in a DSC Q200 differential scanning calorimeter (TA Instruments, New Castle, Delaware, USA).

Thermogravimetric analysis was performed to determine decomposition temperature of the crystals, using a TGA Q5000 series thermogravimetric analyzer (TA Instruments, New Castle, Delaware, USA) with 11.805-23.799 mg crystals each sample. Temperature was increased to 500 °C at a ramping rate of 20 °C/min when nitrogen flow rate was at 10 mL/min. The results were analyzed using TA universal VA.7A thermal analysis software. The decrease of mass remaining with increasing temperature and the rate of mass loss (derivative of mass change with temperature) were compared among the recovered crystals and the reagent grade ammonium sulfate crystals.

3 RESULTS AND DISCUSSION

3.1 Optimum Feed Depth for Vacuum Thermal Stripping

Assuming equilibrium concentration of free ammonia is zero [4, 6], the value of K_La for ammonia mass transfer was estimated for the batch stripping experiments at different feed depths (Table 1). The K_La value for the digested sludge decreased and

the mass of ammonia stripped increased with increasing feed depth. However, the changes of K_{La} , stripping efficiency and mass of ammonia stripped across the three feed depths were statistically insignificant ($P = 0.10, 0.35, 0.17$). As shown in Equation 2, a decrease in K_{La} indicates a proportional increase in the stripping time required to attain a given final ammonia concentration. For a given digestate recirculation rate, a longer stripping time means more strippers to invest on and operate. Based on the decrease rate of K_{La} and the increase rate of ammonia stripped as feed depth was increased from 8.5 to 25.5 cm, it appears that 17 cm is the best feed depth. Detailed economic analysis is needed to identify the optimum feed depth for a given hydraulic capacity and digestate ammonia concentration.

Table 1. Effects of feed depth on vacuum thermal stripping of ammonia in digestate.

Parameter	Feed depth				
	8.5 cm	17.0 cm	25.5 cm	33.5 cm	41.5 cm
<i>Anaerobically digested municipal sludge (Mean ± Standard deviation of 5 batches)</i>					
Digestate ammonia (mg N/L)	1149 ± 56	995 ± 29	1042 ± 38		
Ammonia stripping efficiency, R_e (%)	91.4 ± 12.5	91.6 ± 6.5	74.4 ± 27.3		
Volumetric mass transfer coefficient, K_{La} (1/h)	0.64 ± 0.30	0.54 ± 0.20	0.12 ± 0.07		
Ammonia stripped (g)	9.01 ± 1.36	11.3 ± 0.61	9.55 ± 3.18		
<i>Anaerobically digested dairy manure (Mean ± Standard deviation of 5 batches)</i>					
Digestate ammonia (mg N/L)	1830 ± 117	2150	2175		
Ammonia stripping efficiency, R_e (%)	92.2 ± 7.8	76.3	47.4		
Volumetric mass transfer coefficient, K_{La} (1/h)	0.56 ± 0.16	0.26	0.10		
Ammonia stripped (g)	14.3 ± 1.97	27.7	26.1		

Compared with vacuum thermal stripping of digested dairy manure in a 2-L flask at feed depth less than 3.8 cm, which removed 99.9% ammonia in 3 h [4], stripping in the pilot system at feed depths of 8.5-25.5 cm removed 47.4-92.2% ammonia in 5 h (Table 1). When digested dairy manure was stripped in the flask at feed depth less than 3.8 cm, the average K_{La} value was as high as 1.83 h^{-1} [4]. The K_{La} value for digested dairy manure decreased steeply as feed depth was increased up to 25.5 cm. Based on the percentages of decrease in K_{La} and increase in the mass of ammonia stripped, 17 cm is the best feed for digested dairy manure, which coincides with that for digested sludge.

The digested sludge had greater K_{La} values than the digested dairy manure at each feed depth (Table 1), which could be attributed to the difference in dissolved solids concentration. Unlike water-ammonia binary systems, digestate has diverse constituents with high suspended and dissolved solids concentrations. Apparent

viscosity of liquid manure increases with total solids concentration [14]. Fernández et al. [15] found a non-linear decrease of ammonia mass transfer efficiency with increasing apparent viscosity in digested sewage sludge. Vaddella et al. [16] reported a decrease of overall ammonia transfer coefficient with increasing total solids content of liquid dairy manure because ammonia may act as a ligand to complex with the high concentrations of metals such as Mg^{2+} and Ca^{2+} in digestate and form metal ammine complexes [6].

3.2 Sodium Hydroxide Dose for pH Elevation

As shown in Table 2, digestate needs pH elevation for vacuum thermal stripping. The dose begins to increase steeply as pH increases above 9 (Fig. 3). It's hence cost-effective to set pH at 9 for vacuum thermal stripping. The dose of NaOH for increasing digestate pH to 10 could be well simulated with 2- or 3-order polynomial equations (coefficient of determination $R^2 \geq 0.996$). The dosing curves varied over time and especially among the three types of digestate. NaOH doses for the digested dairy manure were higher than those for the digested sludge and co-digested foodwaste.

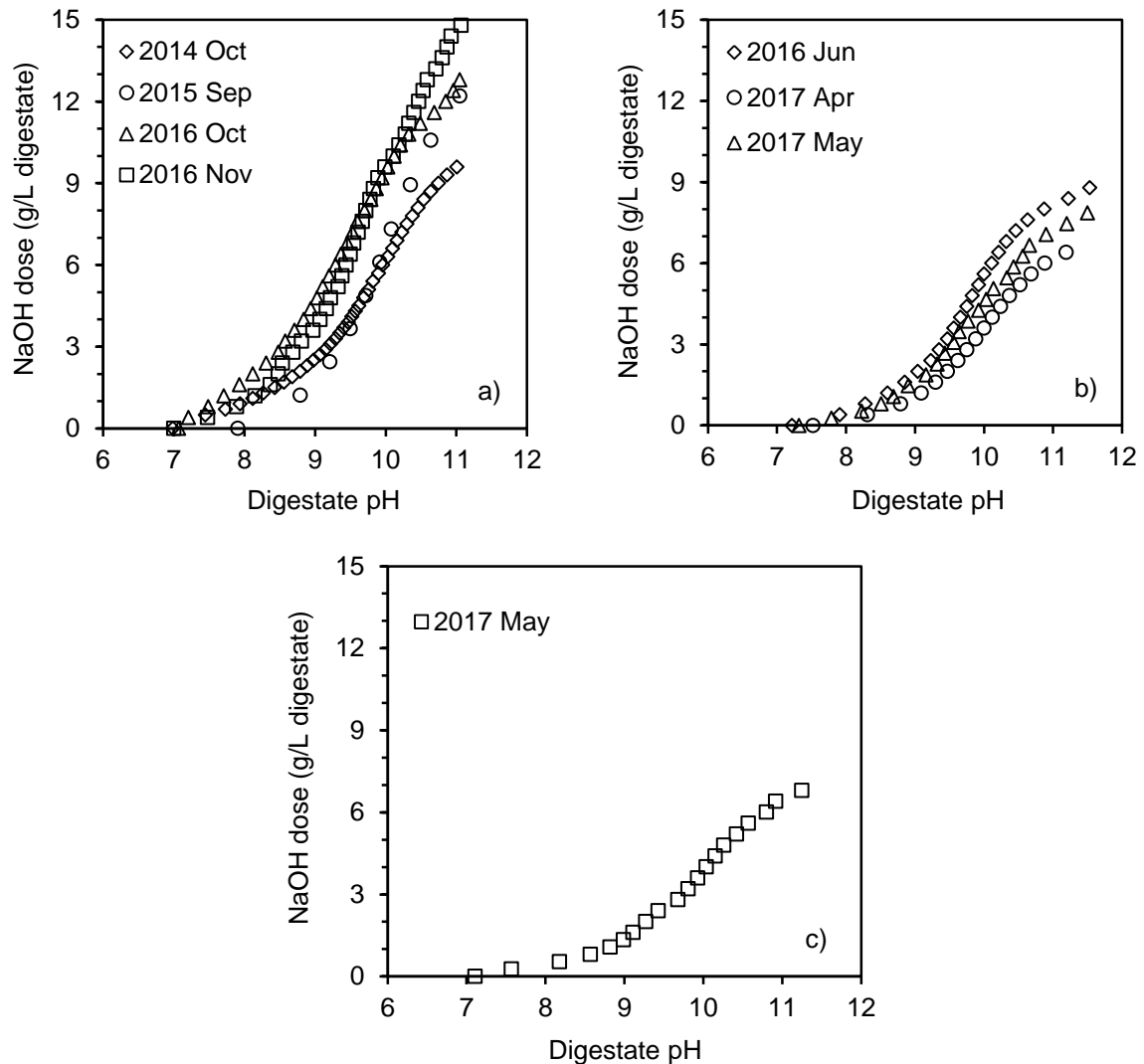


Fig. 3 NaOH dosing curves for a) digested dairy manure, b) digested sludge, and c) co-digested foodwaste and dairy manure

Table 2. Properties of digestate used to develop sodium hydroxide dosing curves (Mean \pm Standard deviation).

Digestate	Digested dairy manure	Digested municipal sludge	Co-digested foodwaste
pH	7.24 \pm 0.45	7.35 \pm 0.15	7.11
Ammonia (mg N/L)	1604 \pm 349	1149 \pm 178	1119
Total solids (mg/L)	52.71 \pm 12.32	12.66 \pm 3.17	21.84
Total dissolved solids (mg/L)	10.97 \pm 0.55	4.89 \pm 0.64	8.05
Dose for pH 9 (g NaOH/L)	3.21 \pm 1.37	1.55 \pm 0.42	1.38
Dose from pH 8 to 9 (g NaOH/L)	2.33 \pm 0.83	1.25 \pm 0.20	1.01

Digestate has high concentrations of ammonium, phosphates and alkalinity [17]. In the pH range of 7 and 9, dynamic equilibrations of the ammonia species (NH_4^+ , NH_3), phosphate species (HPO_4^{2-} , H_2PO_4^-), and carbonate species (CO_3^{2-} , HCO_3^- , H_2CO_3) affect NaOH dose. Therefore, both the doses to increase pH from 8 to 9 and attain pH 9 had strong correlations with total dissolved solids concentration (correlation coefficient $r = 0.84$ and 0.76) and TAN concentration ($r = 0.84$ and 0.74).

3.3 Thermal Stability of Recovered Ammonium Crystals

Ukwuani and Tao [4] have reported the ammonium sulfate content of the crystals recovered earlier from foodwaste digestate and reverse osmosis retentate of landfill leachate to be 100.0-102.3% and 94.3-106.8%, respectively. The heat flow traces from the DSC analysis (Fig. 4) indicated that the crystals melted at 291.4 and 293.5 °C, whereas the reagent grade crystals melted at 295.9 °C. A melting point of 295 °C has been reported by Mohan et al. [18] for $(\text{NH}_4)_2\text{SO}_4$ crystals produced from a supersaturated solution of ammonium sulfate. Ammonium sulfate has been reported to melt with decomposition at temperatures 235-356 °C [19-24]. The variation of the melting point in the literature is primarily attributed to incorrect experimental techniques performed in some previous studies [21]. The suspected impure ammonium compounds in the recovered crystals have melting points lower than that of ammonium sulfate. For example, the melting point of ammonium bisulfate is 139–147 °C [20, 21, 23, 24], triammonium hydrogen disulfate 225–234 °C [21, 23-25], ammonium bicarbonate 107 °C [20], and ammonium carbonate 58 °C [20]. Therefore, the measured melting point of the recovered crystals and its similarity to the melting point of the reagent grade crystals confirmed the production of ammonium sulfate as crystals.

The thermogravimetric analysis indicated a two-stage weight loss (Fig. 5 and Fig. S1), which is typical for thermal decomposition of ammonium sulfate involving the first-stage decomposition to ammonium bisulfate due to loss of ammonia and the second-stage decomposition of ammonium bisulfate to ammonium pyrosulfate and gases [26, 27]. The weight loss profiles showed 16.62% and 17.15% of weight loss in the first-stage decomposition for the recovered crystals at the temperatures of 375 °C and 362

°C respectively, compared with a weight loss of 17.81% at 350 °C for the reagent grade crystals. Stoichiometrically, the complete decomposition of ammonium sulfate to ammonium bisulfate results in a mass loss of 12.87%. The higher weight loss observed than the stoichiometric percentage of complete first-stage decomposition could be attributed to the lower decomposition temperature of ammonium bisulfate and H₂O release. The recovered crystals began to decompose at temperatures approximately 230 and 225 °C, compared with approximately 225 °C at which the reagent grade crystals began to decompose, similar to those reported by Song et al. [26], Petkova et al. [22], Galwey and Brown [27] and Thege [23, 24]. The mass loss due to decomposition reached more than 99.6% at 462 °C and 447 °C for the recovered crystals, compared with 450 °C for the reagent grade crystals. These values are close to those reported by Kandil et al. [19] and Galwey and Brown [27] for pure ammonium sulfate.

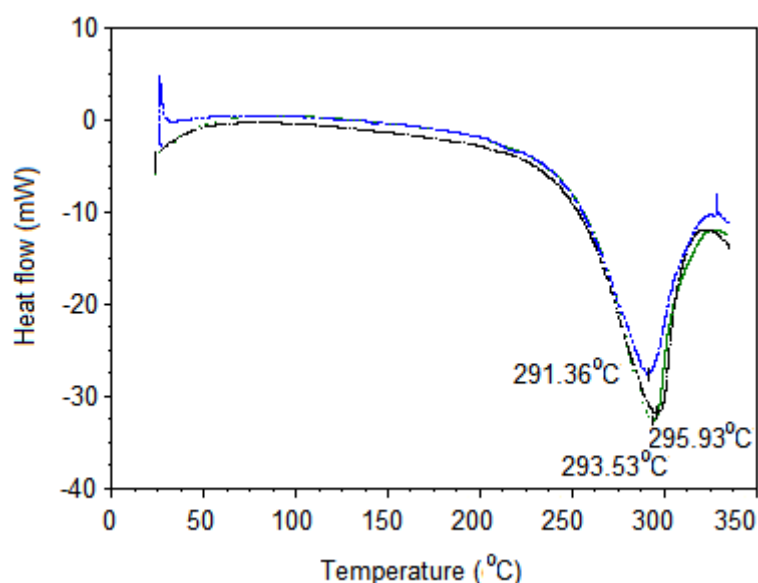
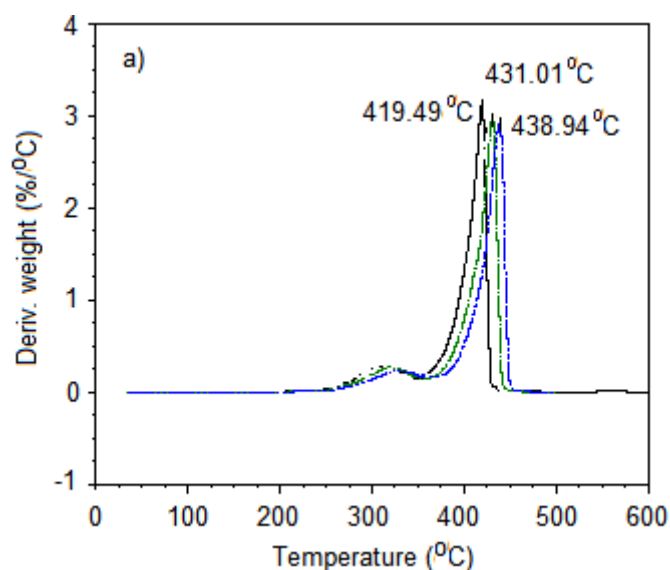


Fig. 4 Overlay of differential scanning calorimetry traces for comparing the melting points of the crystals recovered from foodwaste digestate (blue curve), the crystals recovered from reverse osmosis retentate of landfill leachate (green curve), and reagent grade ammonium sulfate crystals (black curve)



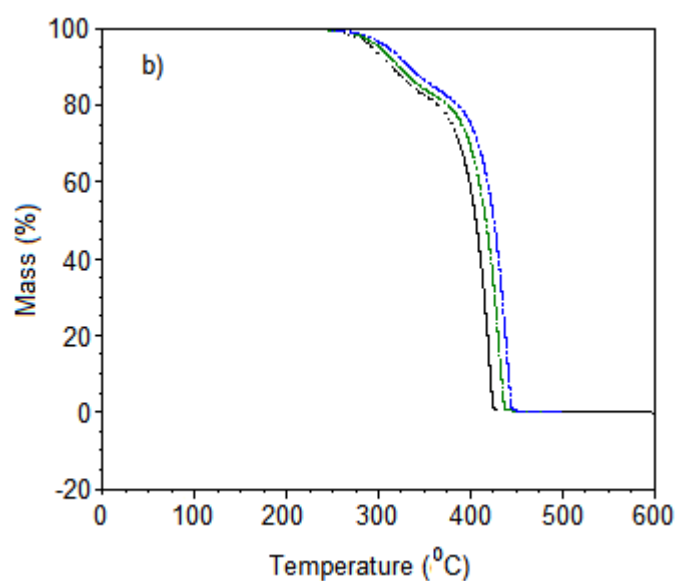


Fig. 5 Overlay of thermograms in a) rate of mass loss and b) percentage of mass remaining for comparing decomposition of the crystals recovered from foodwaste digestate (blue lines), crystals recovered from reverse osmosis retentate of landfill leachate (green lines), and reagent grade ammonium sulfate crystals (black lines)

Given the observed thermal properties of the recovered crystals with reference to the reagent grade ammonium sulfate crystals in addition to earlier chemical analysis, the recovered crystals are $(\text{NH}_4)_2\text{SO}_4$ with possibly a small portion of impure compounds. As indicated by Ukwuani and Tao [4], the impurity can be decreased by better control of sulfuric acid content in the absorption solution. The other impurity such as metals may originate from sulfuric acid to be used for gas absorption. More physical and chemical properties of the recovered crystals need to be determined in order to place the product as a cheaper fertilizer or high-value reagent grade chemical.

Acknowledgments

This study was supported by an U.S. Environmental Protection Agency grant to Dr. Tao (SU835937). The views expressed in this document are solely those of the authors and do not necessarily reflect those of the Agency.

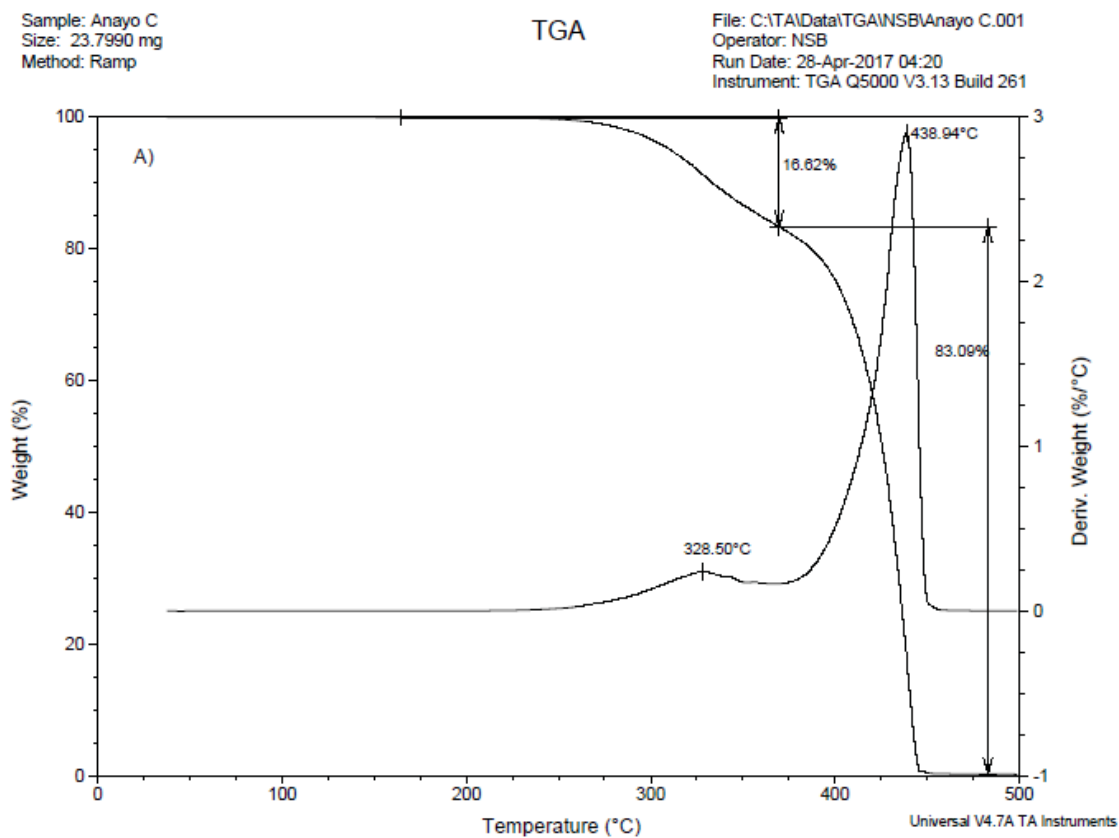
References

- [1] Cook, S.M., Skerlos, S.J., Raskin, L., Love, N.G.: A stability assessment tool for anaerobic codigestion. *Water Res.* 112, 19–28 (2017)
- [2] Rajagopal, R., Masse, D.I., Singh, G. A critical review on inhibition of anaerobic digestion process by excess ammonia. *Bioresour. Technol.* 143, 632–41 (2013)
- [3] Yenigun, O., Demirel, B.: Ammonia inhibition in anaerobic digestion: A review. *Process Biochem.* 48, 901–911 (2013)

- [4] Ukwuani, A., Tao, W.: Developing a vacuum thermal stripping - acid absorption process for ammonia recovery from anaerobic digester effluent. *Water Res.* 106, 108–115 (2016)
- [5] Anwar, S.W., Tao, W.: Cost benefit assessment of a novel thermal stripping - acid absorption process for ammonia recovery from anaerobically digested dairy manure. *Water Prac. Technol.* 11, 355–364 (2016)
- [6] Tao, W., Ukwuani, A.T.: Coupling thermal stripping and acid absorption for ammonia recovery from dairy manure : Ammonia volatilization kinetics and effects of temperature, pH and dissolved solids content. *Chem. Eng. J.* 280, 188–196 (2015)
- [7] Vrieze, J.D., Smet, D., Klok, J., Colsen, J., Angenent, L.T., Vlaeminck, S.E.: Thermophilic sludge digestion improves energy balance and nutrient recovery potential in full-scale municipal wastewater treatment plants. *Bioresour. Technol.* 218, 1237–1245 (2016)
- [8] Jiang, A., Zhang, T., Zhao, Q.-B., Li, X., Chen, S., Frear, C.S.: Evaluation of an integrated ammonia stripping, recovery, and biogas scrubbing system for use with anaerobically digested dairy manure. *Biosys. Eng.*, 119, 117–126 (2014)
- [9] Zarebska, A., Romero Nieto, D., Christensen, K.V., Norddahl, B.: Ammonia recovery from agricultural wastes by membrane distillation: Fouling characterization and mechanism. *Water Res.* 56, 1–10 (2014)
- [10] Ledda, C., Schievano, A., Salati, S., Adani, F.: Nitrogen and water recovery from animal slurries by a new integrated ultrafiltration, reverse osmosis and cold stripping process: A case study. *Water Res.* 47, 6157–6166 (2013)
- [11] Morales, N., Boehler, M.A., Buettner, S., Liebi, C., Siegrist, H.: Recovery of N and P from urine by struvite precipitation followed by combined stripping with digester sludge liquid at full scale. *Water* 5, 1262–1278 (2013)
- [12] Dingle, N., Bhanuprasad, M.: Ammonium sulfate crystallization in Andersen cascade impactor samples. *Atmos. Environ.* 8, 1119–1130 (1974)
- [13] APHA, AWWA, WEF: *Standard Methods for the Examination of Water and Wastewater*, twenty-second ed. American Public Health Association/American Water Works Association/Water Environment Federation, Washington, DC (2012)
- [14] Bhaga, D., Weber, M.E.: Bubbles in viscous liquids: shapes, wakes and velocities. *J. Fluid Mech.* 105, 61–85 (1981)
- [15] Fernández, Y.B., Cartmell, E., Soares, A., McAdama, E., Vale, P., Darce-Dugaret, C., Jefferson, B.: Gas to liquid mass transfer in rheologically complex fluids. *Chem. Eng. J.* 273, 656–667 (2015)
- [16] Vaddella, V.K., Ndegwa, P.M., Ullman, J.L., Jiang, A.: Mass transfer coefficients of ammonia for liquid dairy manure. *Atmos. Environ.* 66, 107–113 (2013)
- [17] Tao, W., Fattah, K.P., Huchzermeier, M.P.: Struvite recovery from anaerobically digested dairy manure: A review of application potential and hindrances. *J. Environ. Manag.* 169, 46–57 (2016)

- [18] Mohan, R., Kaytancioglu, O., Myerson, A.S.: Diffusion and cluster formation in supersaturated solutions of ammonium sulfate at 298 K. *J. Cryst. Growth* 217, 393–403 (2000)
- [19] Kandil, A.T., Cheira, M.F., Gado, H.S., Soliman, M.H., Akl, H.M.: Ammonium sulfate preparation from phosphogypsum waste. *J. Radiat. Res. Appl. Sci.* 10, 24–33 (2017)
- [20] Haynes, W. (ed.): *CRC Handbook of Chemistry and Physics*, 97th ed. CRC Press, Boca Raton, FL (2016)
- [21] Kosova, D.A., Emelina, A.L., Bykov, M.A.: Phase transitions of some sulfur-containing ammonium salts. *Thermochim. Acta* 595, 61–66 (2014)
- [22] Petkova, V., Pelovski, Y., Hristova, V.: Thermal analysis for identification of E-Beam nanosize ammonium sulfate. *J. Therm. Anal. Calorim.* 82, 813–817 (2005)
- [23] Thege, I.K.: DSC investigation of the thermal behaviour of $(\text{NH}_4)_2\text{SO}_4$, NH_4HSO_4 and $\text{NH}_4\text{NH}_2\text{SO}_3$. *Thermochim. Acta* 60, 149–159 (1983a)
- [24] Thege, I.K.: DSC studies of binary inorganic ammonium compound systems. *J. Therm. Anal.* 27, 275–286 (1983b)
- [25] Kwak, H., Hwang, D.W., Hwang, Y.K., Chang, J.-S.: Recovery of alkyl lactate from ammonium lactate by an advanced precipitation process. *Sep. Purif. Process* 93, 25–32 (2012)
- [26] Song, X., Zhao, J., Li, Y., Sun, Z., Yu, J.: Thermal decomposition mechanism of ammonium sulfate catalyzed by ferric oxide. *Front. Chem. Sci. Eng.* 7, 210–217 (2013)
- [27] Galwey, A.K., Brown, M.E. (eds.): *Thermal Decomposition of Ionic Solids*. Elsevier Science, Amsterdam (1999)

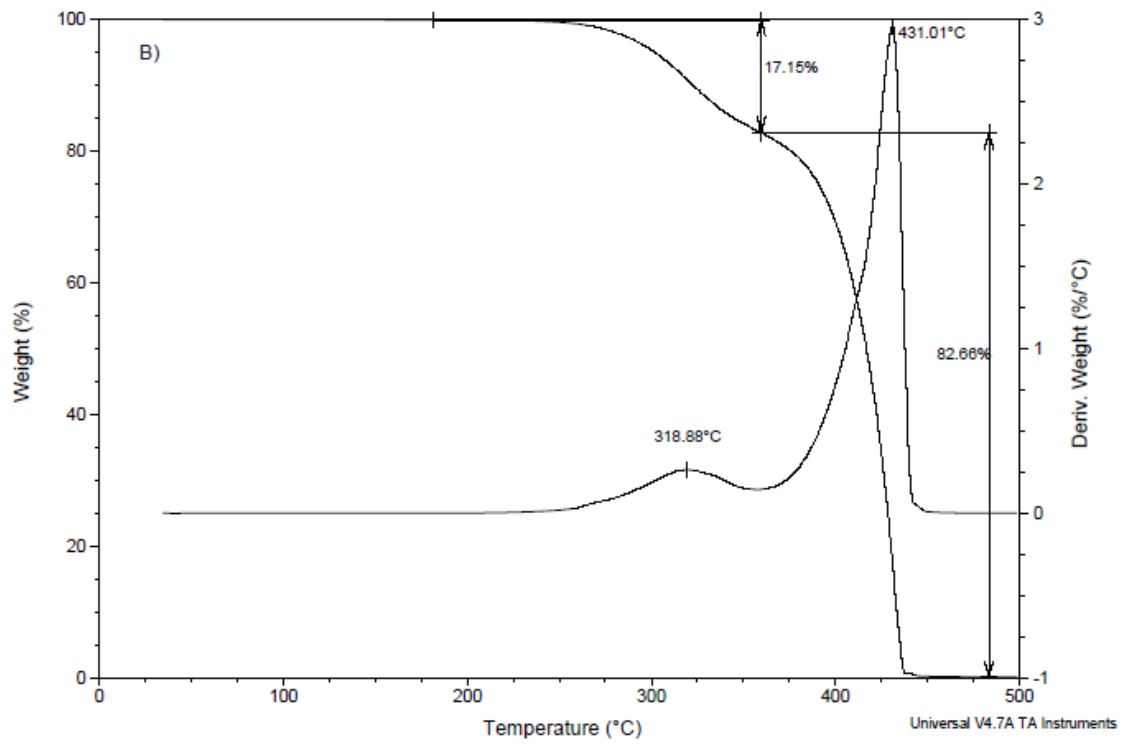
Fig. S1 Thermogravimetric analysis traces of mass (%) and rate of mass loss (%/°C) for A) the crystals recovered from foodwaste digestate, B) the crystals recovered from reverse osmosis retentate of landfill leachate, and C) reagent grade ammonium sulfate crystals. The thermogravimetric analyzer was run at a temperature ramping rate of 20 °C/min and nitrogen flow rate of 10 mL/min.



Sample: Anayo D
Size: 16.9060 mg
Method: Ramp

TGA

File: C:\TAIData\TGAINSB\Anayo D.001
Operator: NSB
Run Date: 28-Apr-2017 03:32
Instrument: TGA Q5000 V3.13 Build 261



Sample: Anayo STD
Size: 11.8050 mg
Method: Ramp

TGA

File: C:\TAIData\TGAINSB\Anayo STI
Operator: NSB
Run Date: 28-Apr-2017 01:33
Instrument: TGA Q5000 V3.13 Build 2

